www.czasopisma.pan.pl PAN POLSKA AKADEMIA NAUK www.journals.pan.pl

Arch. Metall. Mater. **65** (2020), 2, 959-966

DOI: 10.24425/amm.2020.132844

P. GOGOLA[1], Z. GABALCOVÁ[1], H. SUCHÁNEK[1], M. BABINEC[1], M. BONEK[2], M. KUSÝ[1*]

QUANTITATIVE X-RAY DIFFRACTION ANALYSIS OF Zn-Al BASED ALLOYS

The paper describes modification to Fm$\bar{3}$m (space group no. 225) lattice of aluminium based α-solid solution observed in Zn-Al alloys required to properly correlate quantitative data from X-ray diffraction analysis with results obtained from quantitative scanning electron microscopy image analysis and those predicted from Zn-Al binary phase diagram. Results suggests that 14 at.% of Zn as a solute atom should be introduced in crystal lattice of aluminium to obtain correct estimation of phase quantities determined by quantitative X-ray diffraction analysis. It was shown that this modification holds for Cu mould cast as well as annealed and water-cooled samples of Zn-3wt.%. Al and Zn-5wt.% Al.

Keywords: hot-dip coating, quantitative x-ray diffraction, image analysis, Zn-Al alloy

1. Introduction

Binary Zn-Al alloy systems are known for their broad application in the field of corrosion protection of steel articles. In general, the protective coating layer is formed on a steel surface using a hot-dip coating process where steel articles are dipped in molten Zn-based alloy and held at a dipping temperature for a certain time allowing the formation of a desired Zn-based alloy coating [1].

X-ray diffraction (XRD) technique is frequently used for qualitative analysis of phases in Zn-Al based alloy systems and intermetallics formed during hot dip galvanizing on top of steel substrates [2-5]. It plays also an important role in case when the crystallographic orientation of the coating is studied where texture parameters are calculated from experimental diffraction patterns [6-8]. Stability and lifetime of protective Zn-Al coating depends on type of corrosion products evolved during exposure in specific corrosive environment which could be also identified by XRD analysis [9-11]. Rarely, quantitative results are available from XRD analysis of Zn-Al based systems. In these publications the phase fraction is derived from a single peak [4,12] or multi peak approach [13].

In fact, determination of precise quantities of η and α solid solutions requires to consider several aspects of this alloy system. First aspect is that the binary equilibrium Zn-Al phase diagram possesses broad range of solubility of Zn atoms in a series of α, α' and γ solid solutions with Fm$\bar{3}$m crystal lattice up to 82 wt.% of Zn (approx. 66 at.%.) as it is shown in Fig. 1 [14]. Regarding XRD measurements, such behaviour indicated by binary diagram may require specific modification to the Fm$\bar{3}$m crystal lattice of aluminium (α-phase with virtually 0 at.% Zn at room temperature). It is the significantly different value of atomic scattering factors of Al and Zn which leads to a second specific aspect of this alloy system. The lattice of α-phase solid solution represented by Fm$\bar{3}$m (space group no. 225) crystal lattice of aluminium requires modification which should follow actual chemical composition of this phase. Finally, the last aspect of the Zn-Al system is fine eutectoid mixture of η and α particles with typical size below 1 μm. As it is well known such dimensions hinders from using the energy dispersive X-ray analyser (EDX) as a tool for an effective determination of local chemical composition of α-solid solution.

This paper is aimed at the evaluation of η and α solid solution volume fractions in Zn-3 wt.% Al (later only Zn3Al) and Zn-5 wt.% Al (later only Zn5Al) alloys in as-cast and annealed state using full-XRD pattern Rietveld-based approach. This method allows for phase quantity evaluation while other microstructural factors such as chemical composition of evaluated phases, preferred crystallographic orientation, crystallite size and lattice strain are properly considered. Final phase quantity could be therefore understood as a complex value whose precision depends on how other microstructural factors are described.

[1] SLOVAK UNIVERSITY OF TECHNOLOGY, FACULTY OF MATERIALS SCIENCE AND TECHNOLOGY, INSTITUTE OF MATERIALS SCIENCE AND TECHNOLOGY, ULICA JÁNA BOTTU 25, 917 24 TRNAVA, SLOVAKIA
[2] SILESIAN UNIVERSITY OF TECHNOLOGY, FACULTY OF MECHANICAL ENGINEERING, 18 A KONARSKIEGO STR., 44-100 GLIWICE, POLAND

* Corresponding author: martin.kusy@stuba.sk

© 2020. The Author(s). This is an open-access article distributed under the terms of the Creative Commons Attribution-NonCommercial License (CC BY-NC 4.0, https://creativecommons.org/licenses/by-nc/4.0/deed.en which permits the use, redistribution of the material in any medium or format, transforming and building upon the material, provided that the article is properly cited, the use is noncommercial, and no modifications or adaptations are made.

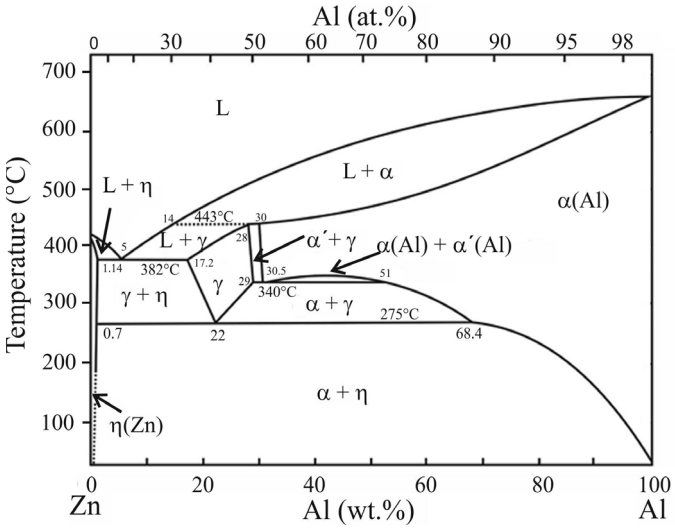

Fig. 1. Binary Zn-Al phase diagram adopted and modified from [15,16]

Values determined from x-ray diffraction analysis are compared with quantitative results from SEM image analysis and with theoretically predicted quantities from equilibrium Zn-Al binary phase diagram.

2. Experimental

Binary Zn3Al and Zn5Al alloys were prepared by melting of at least 4N purity elements. Undesired impurities were removed from the molten zinc by applying Zincogen 318 flux before corresponding amount of pre-heated Al pieces were introduced. After homogenisation at 450°C the molten alloy was poured into a Cu crucible with 30 mm in diameter and 15 mm in depth. Rapid solidification in a Cu mould was chosen to achieve best possible homogeneity of castings. The cooling process in the crucible took place rather rapidly which is documented in time-temperature plot in Fig. 2. The cooling curve depicted by solid line corresponds to a thermocouple positioned at the bottom of the Cu crucible in contact with the side-wall. Initial cooling rate of molten alloy before onset of solidification reached approximately 200°C.s^{-1}. Average cooling rate over initial 100°C from the start of solidification was approximately 32°C.s^{-1}. Thermocouple placed at the bottom of the crucible (dotted line in Fig. 1) in the centre of the casting indicated initial cooling rate of approximately 25°C.s^{-1} before solidification onset. Average cooling rate over the range of initial 100°C was approximately 10°C.s^{-1}.

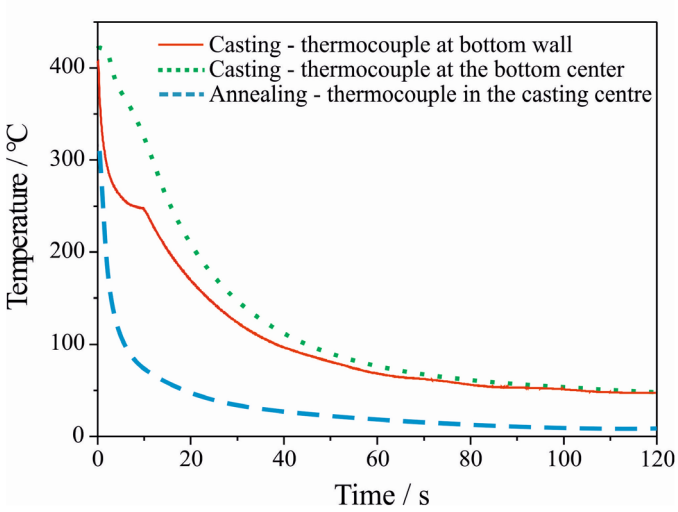

Fig. 2. Time-temperature diagram of cooling from casting and annealing temperature

Both castings were subsequently analysed with Spectruma GDA 750 optical emission spectrometer to confirm bulk chemical composition of alloys. Corresponding results are shown in Table 1.

TABLE 1

Nominal and measured bulk chemical composition of Zn3Al and Zn5Al alloy in as-cast state determined by optical emission spectrometry. Composition was evaluated in both wt.% and at.%

Sample	Nominal content of Al wt. % / at. %	Measured content of Al wt. % / at. %
Zn3Al	3 / 7	3,5 / 8.1
Zn5Al	5 / 11.3	5,2 / 11.7

While a set of Zn3Al and Zn5Al samples was left for analysis in as-cast state, a second set was annealed at 350°C for 24 hours in electric resistance furnace and cooled immediately down by water quenching. The corresponding cooling curve, documented as dashed line in Fig. 2, suggests that average cooling rate over initial 100°C was approximately 65°C.s^{-1}.

Microscopic examination and x-ray diffraction were carried out on metallographically prepared cross-sections. Samples were ground using 220, 600, 1200, 2500 and 4000 grit waterproof abrasive papers. Polishing was executed using alcohol based 3, 1 and 0.25 µm diamond slurry. No etching was applied.

Scanning electron microscope Jeol JSM 7600F (SEM) with Oxford Instruments X-MAX 50 energy dispersive X-ray analyser (EDX) was used to reveal microstructure of as-cast and annealed samples and identify local chemical composition of η-phase and morphologically distinct areas of eutectics and eutectoids. Image analysis was executed on back scattered electron (BSE) SEM images using image analysis program ImageJ [17].

Identification of phases and phase quantity was carried out on PANalytical Empyrean X-ray diffractometer (XRD). Measurements were performed in Bragg-Brentano geometry with Ni filtered Cu-radiation and PIXcel3D position sensitive detector operated in 1D scanning mode. X-ray diffraction data were further analysed qualitatively using PANalytical Xpert High Score program with ICSD database FIZ Karlsruhe. Quantitative results were determined from XRD patterns using Rietveld refinement-based program MAUD version 2.84 [18].

3. Results

Solidification microstructure of as-cast Zn3Al was found to consist from η dendrites surrounded with binary lamellar eutectic

as documented in Fig. 3a. Detail of the former binary eutectic region shown in Fig. 3b reveals that lamellae formed by former γ solid solution were decomposed during eutectoid transformation into a fine, two phase mixture of η and α solid solution. This is in agreement with the binary phase diagram in Fig. 1

Both distinct microstructural components, dendrites and eutectic, were studied using EDX analysis in order to determine their local chemical composition. Results are shown in Fig. 4 and Table 2. Detailed EDX study of fine-grained microstructure of decomposed lamellae was not possible since dimension of grains are well below 1 μm which would significantly alter results of local chemical composition.

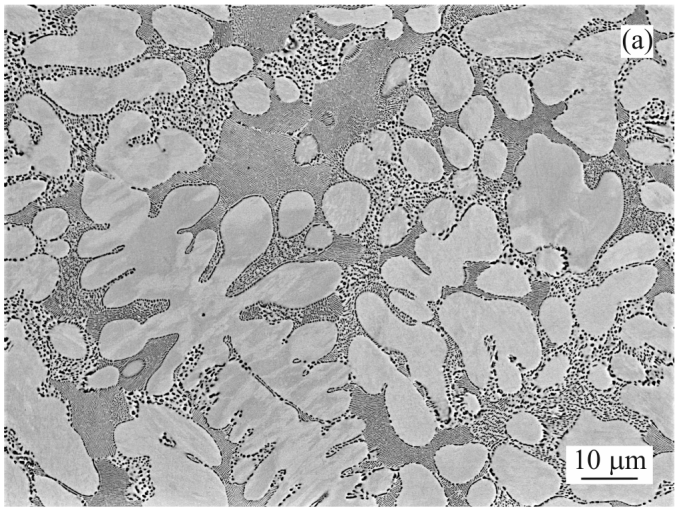

Fig. 3a. Typical solidification microstructure of as-cast Zn3Al, BSE SEM

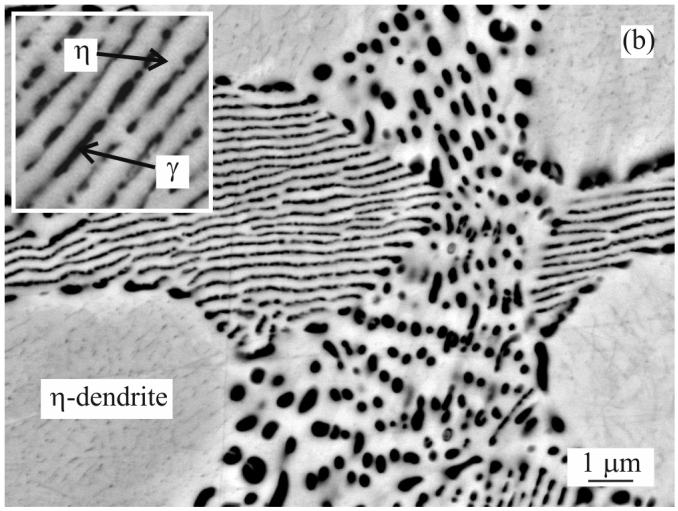

Fig. 3b. Detail of Zn3Al eutectic with former γ phase transformed into a eutectoid mixture of α and η grains, BSE SEM

According to Table 2, as-cast microstructure was found to consist of Zn dendrites containing in average up to 1 wt.% of Al (corresponding to approx. 2 at.% Al). Inter-dendritic eutectic regions were observed to contain typically 94 wt.% of Zn and up to 6 wt.% of Al.

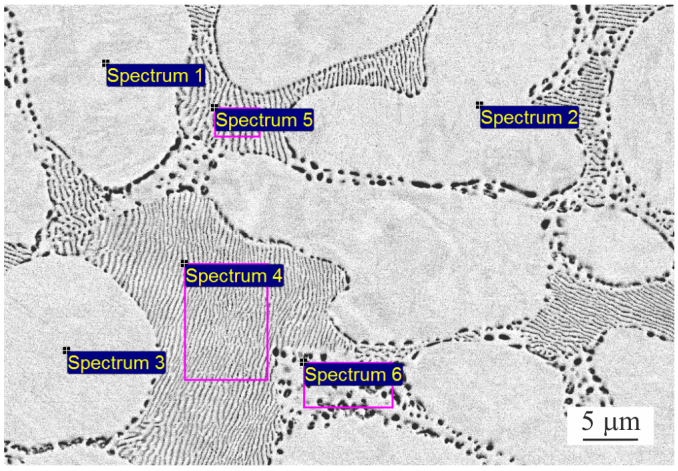

Fig. 4. Local EDX analysis of typical microstructural constituents of as-cast Zn3Al, BSE SEM

TABLE 2

Results of EDX analysis of microstructural constituents of as-cast Zn3Al corresponding to Fig. 4

Spectrum	Al (wt. %) / (at. %)	Zn (wt. %) / (at. %)	Constituent Al average content (wt. %) / (at. %)
Spectrum 1	1.1 / 2.6	98.9 / 97.4	1.1 / 2.5
Spectrum 2	1.1 / 2.6	98.9 / 97.4	
Spectrum 3	1.0 / 2.4	99.0 / 97.6	
Spectrum 4	5.9 / 13.2	94.1 / 86.8	6.1 / 13.7
Spectrum 5	5.9 / 13.2	94.1 / 86.8	
Spectrum 6	6.6 / 14.6	93.4 / 85.4	

As it could be seen from Fig. 5, microstructure of Zn3Al changed significantly upon annealing. Dendritic microstructure was transformed into microstructure containing equiaxed Zn-rich η grains. Eutectic regions located in inter-dendritic areas vanished. Instead, isolated grains composed of fine eutectoid mixture of η and α particles were formed. Fig. 6 and Table 3 documents the chemical composition of microstructural constituents. Equiaxed grains formed by η solid solution were found

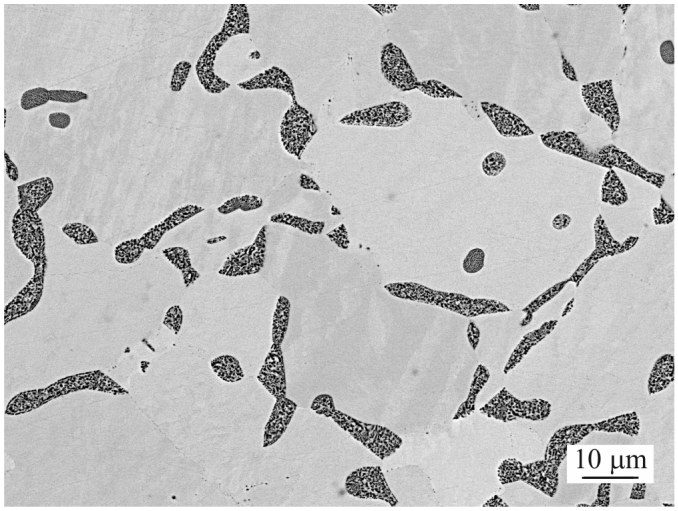

Fig. 5. Typical microstructure of Zn3Al after annealing at 350°C for 24 hours, BSE SEM

to contain 1 wt.% of Al which is the same as in case of as-cast Zn3Al. Eutectoid areas were found to contain in average 19.7 wt.% of Al.

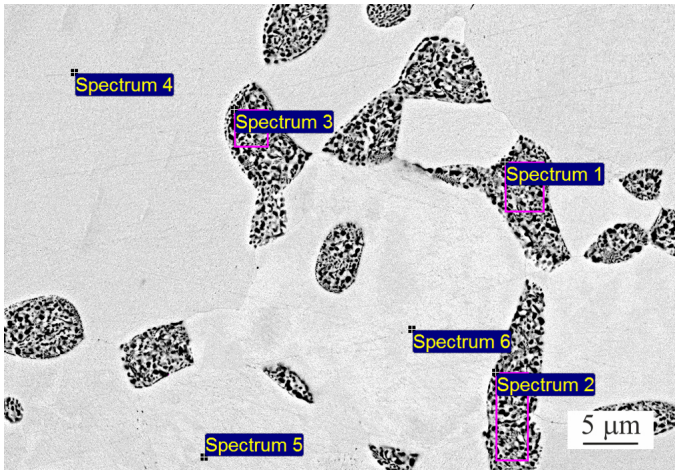

Fig. 6. Local EDX analysis of typical microstructural constituents of as-cast Zn3Al, BSE SEM

TABLE 3

Results of EDX analysis of microstructural constituents of Zn3Al annealed at 350°C for 24 hours, corresponding to Fig. 6

Spectrum	Al (wt. %) / (at. %)	Zn (wt. %) / (at. %)	Constituent average wt. % / at. %
Spectrum 1	21.0 / 39.2	79 / 60.8	22 / 40.9
Spectrum 2	23.4 / 42.5	76.6 / 57.5	
Spectrum 3	22.3 / 41	77.7 / 59	
Spectrum 4	1.1 / 2.6	98.9 / 97.4	1.3/3.1
Spectrum 5	1.1 / 2.6	98.9 / 97.4	
Spectrum 6	1.7 / 4.0	98.3 / 96.0	

Qualitative X-ray diffraction analysis was carried out on both as-cast as well as annealed Zn3Al alloy. Collected X-ray diffraction data are shown in Fig. 7. Two phases, namely, Zn-based $P6_3/mmc$ (space group no. 194 with reference code 98-024-7160) η-solid solution and Al-based $Fm\bar{3}m$ α-solid solution (space group no. 225 with reference code 98-024-0129) were identified and assigned to most intensive peaks.

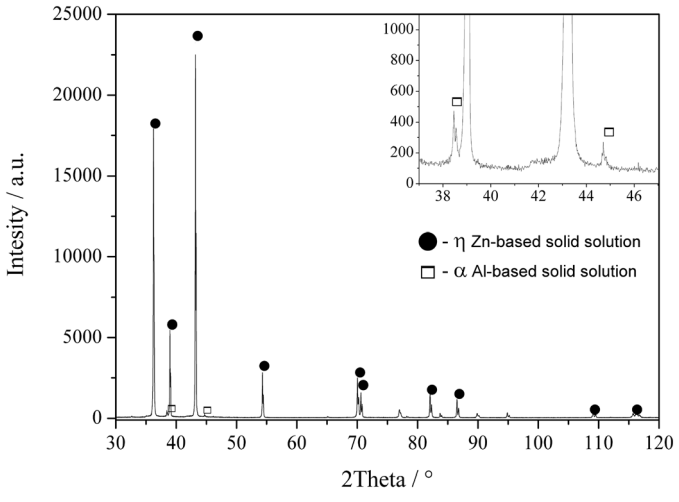

Fig. 7. Qualitative analysis of XRD pattern of as-cast Zn3Al, BSE SEM

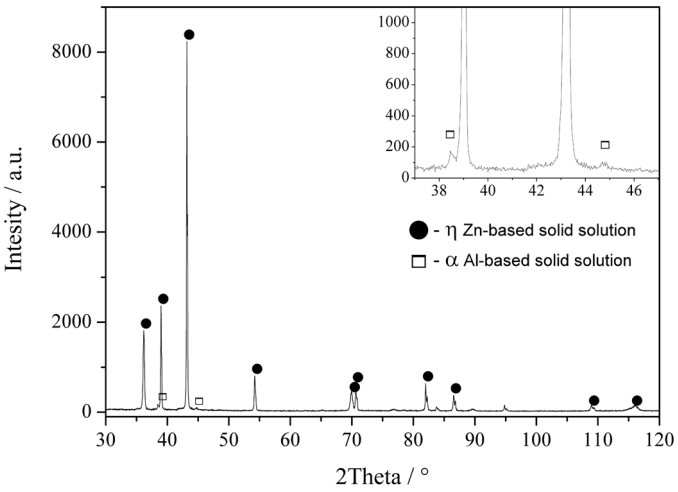

Fig. 8. Qualitative analysis of XRD pattern of Zn3Al annealed for 24 hours at 350°C and water cooled to room temperature, BSE SEM

Contrary to dendritic microstructure of as-cast Zn3Al, the as-cast Zn5Al alloy was found to consist of fully eutectic microstructure. The lamellar microstructure of binary eutectic consists of η lamellae and former γ lamellae transformed into a fine eutectoid mixture of η and α particles (Fig. 9).

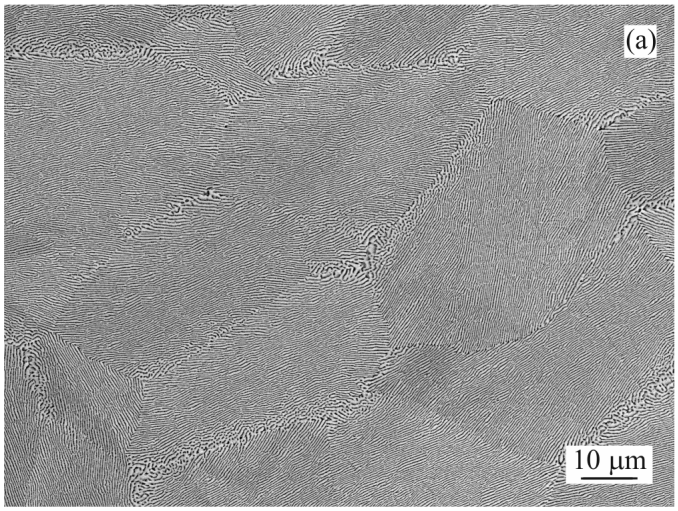

Fig. 9a. Lamellar eutectic microstructure of as-cast Zn5Al alloy, BSE SEM

Appearance of Zn5Al microstructure formed upon 24 hours long annealing at 350°C is depicted in Fig. 10. Eutectic lamellae were replaced with mixture of η grains and islands of former γ phase decomposed into fine eutectoid mixture of η and α particles.

Results of EDX analysis of Zn5Al in as-cast state were not determined due to very fine lamellar morphology. Instead bulk chemical composition determined by optical emission spectrometry in Table 1 is adopted. On the contrary, morphological transformation of microstructure of Zn5Al alloy after annealing

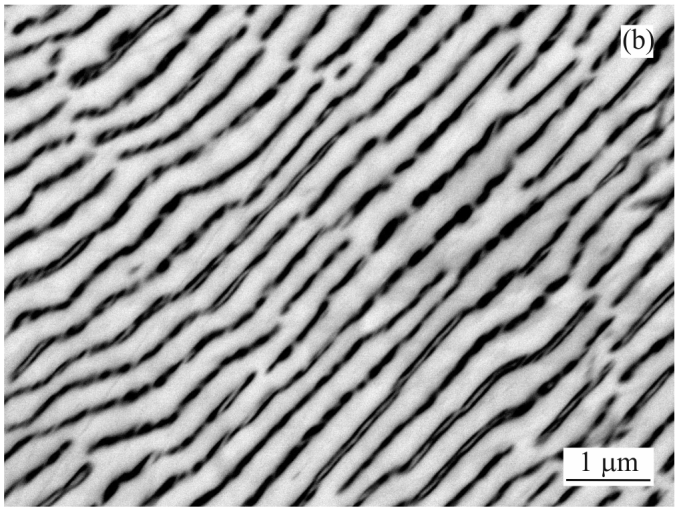

Fig. 9b. Detail of η and former γ lamellae of as-cast Zn5Al, where former γ lamellae is transformed into a fine eutectoid mixture of η and α solid solutions, BSE SEM

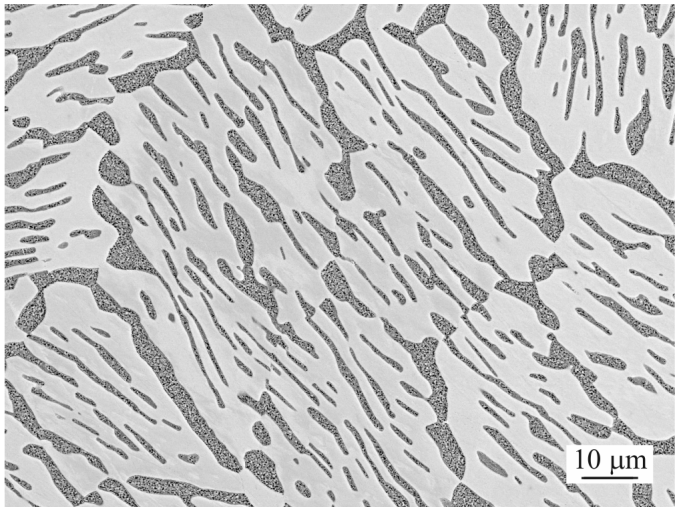

Fig. 10. Microstructure of Zn5Al annealed at 350°C for 24 hours consisting of η grains and islands of former γ phase decomposed into fine eutectoid mixture of η and α particles, BSE SEM

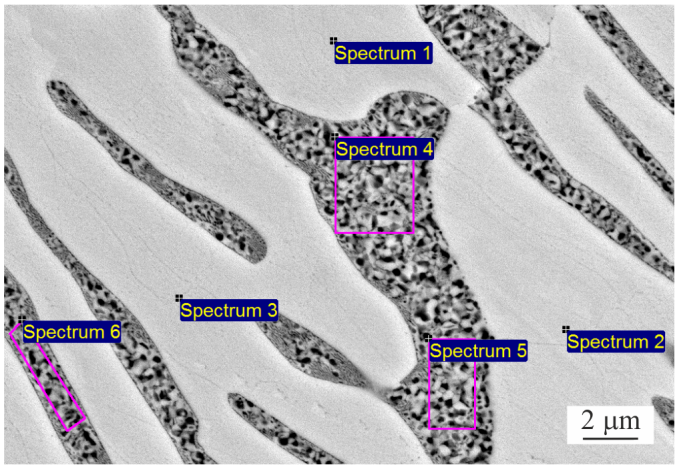

Fig. 11. Local EDX analysis of typical microstructural constituents of Zn5Al after annealing at 350°C for 24 hours and water cooled to room temperature, BSE SEM

allowed for local analysis of chemical composition EDX with results listed in Table 4.

TABLE 4

Results of EDX analysis of microstructural constituents of Zn5Al annealed at 350°C for 24 hours, corresponding to Fig. 11

Spectrum	Al (wt. %) / (at. %)	Zn (wt. %) / (at. %)	Constituent average wt. % / at. %
Spectrum 1	1.2 / 2.9	98.8 / 97.1	1,3 / 3.0
Spectrum 2	1.3 / 3.1	98.7 / 96.9	
Spectrum 3	1.3 / 3.1	98.7 / 96.1	
Spectrum 4	20.5 / 38.5	79.5 / 61.5	19.2 / 36.5
Spectrum 5	17.9 / 34.6	82.1 / 65.4	
Spectrum 6	19.2 / 36.5	80.8 / 63.5	

Results of qualitative XRD phase analysis of Zn5Al alloy in as-cast and annealed state after exposure at 350°C for 24 hours is shown in Fig. 12 and 13. Similarly as in case of Zn3Al and in agreement with binary phase diagram Zn-based $P6_3/mmc$ (space group no. 194 with reference code 98-024-7160) η solid solution was identified. In case of α-solid solution, however, Al-based $Fm\bar{3}m$ α-solid solution with 14 at.% of Zn (space group no. 225 with reference code 98-010-7900) was found to match experimental data better than previously identified Al-based $Fm\bar{3}m$ α-solid solution (space group no. 225 with reference code 98-024-0129).

As-cast condition of the Zn3Al sample shows some differences in the normalized intensities of the diffraction planes compared to database values. Normalized intensities of the planes (0002), $(01\bar{1}0)$ and $(01\bar{1}1)$ have a ratio of $20_{(0002)}$ / $25_{(01\bar{1}0)}$ / $100_{(01\bar{1}1)}$ instead of $35_{(0002)}$ / $24_{(01\bar{1}0)}$ / $100_{(01\bar{1}1)}$. This shows, that the high angle pyramidal plane $(01\bar{1}1)$ [8] is preferred on the surface in contact with the bottom of the Cu mould. This was slightly corrected after annealing, however some texture was maintained, and the ideal normalized intensities were not restored.

Presence of a preferred texture was even more pronounced for the as-cast Zn5Al condition. All three main peaks of the η solid solution were suppressed in favour of the $(11\bar{2}0)$ prismatic plane [8] as shown in Fig. 12 (at approximately 70.5° 2θ). For example, the predicted ratio of $100_{(01\bar{1}1)}$ / $12_{(11\bar{2}0)}$ has changed to $25_{(01\bar{1}1)}$ / $100_{(11\bar{2}0)}$. Annealing at 350°C for 24 hours almost completely vanished the as-cast texture of Zn5Al with ratio changing to $100_{(01\bar{1}1)}$ / $26_{(11\bar{2}0)}$ (Fig. 13).

Results of quantitative image analysis of BSE images are documented in Table 5. Several microstructure images (similar as Fig. 3 to 10) were studied. However, these provide only an opportunity to determine the volume fraction of the former γ-solid solutions. The reason is that lamellae observed within these regions are composed of a fine mixture of η- and α-particles. It is not possible to distinguish and quantify such fine features, while covering a statistically significant area for quantitative analysis. Resulting data on the volume fraction of the former γ-solid solutions can be later recalculated, based on the Zn-Al binary diagram, to indicate the actual volume fraction of η and α-solid solutions.

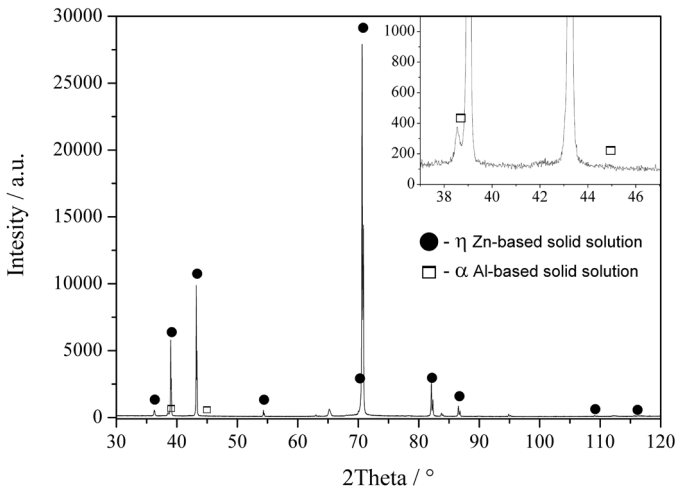

Fig. 12. Qualitative analysis of XRD pattern of as-cast Zn5Al

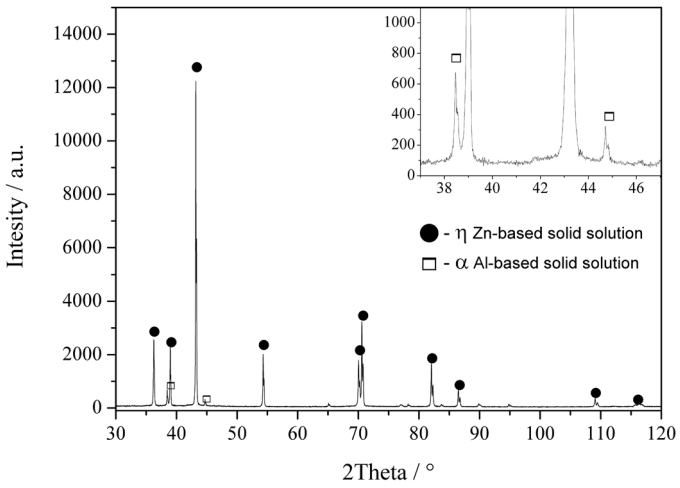

Fig. 13. Qualitative analysis of XRD pattern of Zn5Al annealed for 24 hours at 350°C and water cooled to room temperature

TABLE 5

Quantitative results determined from a series of BSE images of Zn3Al and Zn5Al samples

Treatment	Composition	
	Zn3Al	Zn5Al
Quantitative SEM image analysis of as-cast microstructures	γ = 13.6 ± 4.6 vol.% (balance η = 86.4 vol.%)	γ = 27.3 ± 2.6 vol.% (balance η = 72.7 vol.%)
Quantitative SEM image analysis of samples annealed at 350°C for 24 hours	γ = 12.8 ± 2.1 vol.% (balance η = 87.2 vol.%)	γ =27.5±1.9 vol.% (balance η = 72.5%)

Quantitative XRD analysis was carried in order to determine volume fraction of η and α-solid solutions in Zn3Al and Zn5Al in both, as-cast as well as annealed state. Zn-rich η solid solution was in case of Zn3Al and Zn5Al represented by Zn-based $P6_3/mmc$ (space group no. 194 with reference code 98-024-7160). Al-rich α-solid solution was in case of Zn3Al represented by Al-based $Fm\bar{3}m$ (space group no. 225 with reference code 98-024-0129) where Al occupied 100 at.% with crystallographic data listed in Table 6. In case of Zn5Al the lattice was represented by Al-based $Fm\bar{3}m$ α-solid solution with 14 at.% of Zn (space group no. 225 with reference code 98-010-7900). Crystallographic data of all lattices used for quantitative analysis are summarized in Table 6. Determined results of quantitative XRD analysis are listed in Table 7.

TABLE 6

Review of crystallographic parameters of Zn- and Al-based phases that were found to match experimental XRD data

Phase	Composition	Space group, space group no. and lattice parameters	Reference code
η (Zn)	Zn	$P6_3/mmc$, 196, a = 0.2665 nm c = 0.4962 nm	98-024-7160
α (Al)	Al	$Fm\bar{3}m$, 225, a = 0.4056 nm	98-024-0129
α (Al,Zn)	Al0.86 Zn0.14	$Fm\bar{3}m$, 225 a = 0.4037 nm	98-010-7900

TABLE 7

Quantitative results of full-pattern Rietveld refinement for Zn3Al and Zn5Al in both as-cast as well as in annealed state

Type of sample treatment	Composition	
	Zn3Al	Zn5Al
As-cast samples	α = 9.4 ±0.8 vol.% (balance η = 90.6 vol.%)	α = 12.9±1.2 vol.% (balance η = 87.1 vol.%)
Samples annealed at 350°C for 24 hours	α = 8.5 ±0.9 vol.% (balance η = 87.2 vol.%)	α =12.5±1.2 vol.% (balance η = 87.5%)

4. Discussion

Zn3Al and Zn5Al alloys were prepared by casting into a copper mould. In case of the Zn3Al alloy the typical solidification microstructure was composed of primary η – Zn rich dendrites surrounded by eutectic areas. The fact that eutectoid transformation took place during cooling from casting temperature was confirmed by detailed inspection of as-cast microstructure as shown in Fig. 3b and Fig. 9b. This revealed presence of former γ phase lamellae decomposed into a fine mixture of η and α particles. In agreement with observation of Osorio et al. [19], interdendritic lamellar eutectic mixture has maintained its morphology unaffected, despite the eutectoid transformation. Fully eutectic solidification microstructure was observed in case of Zn5Al alloy which corresponds well with Zn-Al binary phase diagram.

Annealing temperature of 350°C was chosen to correspond with the two phase $\eta + \gamma$ area. Annealing at 350°C for 24 hours led to morphological changes of former solidification microstructures. In case of both alloys equiaxed η (Zn rich) grains were formed, and these were surrounded by former γ grains. These were upon cooling decomposed into a fine grain mixture of α and η. Phase fractions of γ and η at annealing temperature of 350°C are listed in Table 8. Due to water cooling from an-

TABLE 8

Results of phase quantities determined from binary Zn-Al phase diagram. Quantities were determined in wt.% and recalculated to vol.% using known values of phase densities

Quantity of phases determined from Zn-Al binary diagram at temperature	Composition	
	Zn3Al	Zn5Al
350°C	η = 88.5 wt.%; γ = 11.5 wt.% η = 85 vol.%; γ = 15 vol.%	η = 77 wt.%; γ = 23 wt.% η = 72 vol.%; γ = 28 vol.%
276°C	η = 89 wt.%; γ = 11 wt.% η = 85 vol.%; γ = 15 vol.%	η = 80 wt.%; γ = 20 wt.% η = 74 vol.%; γ = 26 vol.%
274°C	η = 96.6 wt.%; α = 3.4 wt.% or η = 93 vol.%, α = 7 vol.%	η = 93.6 wt.%; α = 6.4 wt.% η = 87.2 vol.%, α = 12.8 vol.%

nealing temperature it was assumed that there will be no significant change in phase fractions as consequence of solubility change between 350 and 276°C. However, even in case of slow cooling corresponding to equilibrium Zn-Al phase diagram the estimated 23 wt.% γ at 350°C would decrease only by 3 wt.% to 20 wt.% at 276°C.

At 275°C and eutectoid transformation takes place in Zn-Al binary phase diagram. Bellow this temperature former γ solid solution is decomposed into fine-grain mixture of α a η solid solutions.

Phase fractions of γ, α and η solid solutions were determined for both alloys and three temperatures (350, 276 and 274°C) from the Zn-Al binary phase diagram. Corresponding phase fractions in vol.% were calculated from known wt.% and density of each phase. These values are listed in Table 8 in wt.%.

Quantitative results of SEM BSE image analysis summarized in Table 9 are representing volume fractions of η and γ solid solutions. Phase fraction of η and α for Zn3Al and Zn5Al was subsequently determined from equilibrium α and η phase fraction at eutectoid concentration at 274°C. Comparison of phase fractions predicted from equilibrium Zn-Al phase diagram and those from image analysis allows to conclude that phase fractions of α a η are in good agreement.

A partial agreement is observed. when phase quantity data determined from XRD analysis shown in Table 7 are compared with those predicted by binary phase diagram from Table 8. Quantities predicted from binary diagram (Table 8) and those determined from SEM BSE image analysis (Table 9) are in good agreement with XRD quantitative results of Zn5Al only (Table 7). This could be explained by the fact that α-Al rich solid solution was represented by Fm$\bar{3}$m Al lattice with 14 at.% of Zn. This was not true for Zn3Al alloy where only pure Al and corresponding lattice was used to represent α phase. To confirm this hypothesis quantitative analysis of Zn5Al as-cast sample was executed with Fm$\bar{3}$m Al lattice without Zn solute, in another words with Fm$\bar{3}$m Al lattice with 0 at.% of Zn. It is clear from Table 10 (first row) that determined quantitative results of α-phase were significantly exaggerated, exceeding 18 vol. %.

After applying the same Fm$\bar{3}$m Al lattice with 14 at.% to Zn3Al XRD diffraction pattern refinement the amount of α phase was determined at the level of 6.7 vol.% (Table 10, second row) which is in good agreement with expected values for this composition. Similarly, good agreement was achieved in quantity of α-solid solution determined for samples annealed at 350°C, as well (Table 10, third row). All quantitative results for annealed samples are summarized in Table 10.

TABLE 9

Results of phase quantities determined from quantitative SEM image analysis. All results are given in vol.%

Type of sample treatment	Composition	
	Zn3Al	Zn5Al
As-cast microstructures	γ = 13.6 ± 4.6 vol.% which corresponds to η = 93.2 vol.%; α = 6.8 vol.%	γ = 27.3 ± 2.6 vol.% which corresponds to η = 86.3 vol.%; α = 13.7 vol.%
Annealed at 350°C for 24 hours	γ = 12.8 ± 2.1 vol.% which corresponds to η = 93.6 vol.%; α = 6.4 vol.%	γ = 27.5±1.9 vol.% which corresponds to η = 86.2 vol.%; α = 13.8 vol.%

TABLE 10

Results of phase quantities determined from quantitative Rietveld analysis. All results are given in vol.% only

Type of sample treatment	Composition	
	Zn3Al	Zn5Al
As-cast samples – α solid solution represented by Al lattice (without Zn solute)	α = 9.4±0.8 vol.% (balance η = 90.6 vol.%)	α = 18.2±1.1 vol.% (balance η = 81.8 vol.%)
As-cast samples – α solid solution represented by Al lattice containing 14 at. % of Zn	α = 6.7±0.7 vol.% (balance η = 93.3 vol.%)	α = 12.9±1.2 vol.% (balance η = 87.1 vol.%)
Annealed at 350°C for 24hours – α solid solution represented by Al lattice containing 14 at. % of Zn	α = 6.2±0.7 vol.% (balance η = 93.8 vol.%)	α =12.5±1.2 vol.% (balance η = 87.5%)

5. Conclusions

Binary Zn3Al and Zn5Al alloy samples were prepared in as-cast state by casting into a copper mould and also by annealing at 350°C for 24 hours. These four groups of samples were studied using quantitative SEM image analysis and full-XRD pattern Rietveld refinement technique with the aim to compare quantity of α and η solid solutions. Experimentally determined values were also confronted with prediction determined from binary Zn-Al phase diagram.

Major findings could be summarized as follows:

- Casting into Cu mould led to the formation of preferred grain orientation of $(11\bar{2}0)$ prismatic planes at the expense of high angle pyramidal $(01\bar{1}1)$ planes. This was more pronounced with Al content increasing from 3 to 5 wt.%.
- Annealing at 350°C for 24 hours suppressed the as-cast texture but the random grain orientation distribution was not fully restored.
- Phase quantities determined from quantitative SEM image analysis and binary phase diagram data were found in good agreement.
- Quantities of α and η solid solutions determined by XRD measurements are in rather good agreement with results from quantitative SEM image analysis and binary phase diagram data providing the α-Al rich solid solution is represented in the Rietveld refinement by an Al-based $Fm\bar{3}m$ α-solid solution with 14 at.% of Zn.
- In case the substitution of Al by Zn atoms is not introduced to the Al lattice the estimated quantity of α-Al rich solid solution could be exaggerated by as much as approx. 30 vol.%.
- Substitution of Al by Zn atoms at the level of 14 at.% indicates that diffusion-controlled redistribution of Zn atoms is ceased soon after the eutectoid transformation. The maximum solubility of Zn in α-Al rich solid solution at the eutectoid temperature is found approximately 16 at.%.
- Determination of volume fraction of α-Al rich solid solution using quantitative XRD analysis could achieve comparable precision as in case of microscopic image analysis.
- The advantage of quantitative XRD analysis is the direct quantification of α-Al rich solid solution which is not possible with microscopic methods. Particularly, fine mixture of phases in monotectoid areas are difficult to resolve.
- Disadvantage of quantitative XRD analysis is the necessity to determine the amount of Zn solute in α-Al rich solid solution

Acknowledgement

The authors would like to acknowledge financial support provided by Slovak Grant Agency in the frame of the project VEGA 1/0490/18. The publication is also result of cooperation within the Visegrad Scholarship Program. The publication was co-financed from the statutory grant of the Faculty of Mechanical Engineering at the Silesian University of Technology in 2019

REFERENCES

[1] A.R. Marder, Prog. Mater. Sci. **45** (3), 191-271 (2000).
[2] M. Dutta, S.B. Singh, A.K. Halder, Surf. Coat. Tech. **205** (7), 2578-2584 (2010), DOI: 10.1016/j.surfcoat.2010.10.006.
[3] E. McDevitt, Y. Morimoto, M. Meshii, ISIJ Int. **37** (8), 776-782 (1997).
[4] J.N. Kim, C.S. Lee, Y.S. Jin, Met. Mater. Int. **24** (5), 1090-1098 (2018), DOI: 10.1007/s12540-018-0119-2.
[5] K. Honda, W. Yamada, K. Ushioda, Mater. Trans **49** (6), 1395-1400 (2008).
[6] M.R. Toroghinejad, F. Ashrafizadeh, ISIJ Int. **47** (10), 1510-1517 (2007).
[7] M. Safaeirad, M.R. Toroghinejad, F. Ashrafizadeh, J. Mater. Process. Tech. **196** (1-3), 205-212 (2008), DOI: 10.1016/j.jmatprotec.2007.05.035.
[8] H. Asgari, M.R. Toroghinejad, M.A. Golozar, ISIJ Int. **48** (5), 628-633 (2008).
[9] M.S. Azevedo, C. Allély, K. Ogle, P. Volovitch, Corros. Scie. **90** (C), 472-481 (2015), DOI: 10.1016/j.corsci.2014.05.014.
[10] N.Y. Tang, Y. Liu, ISIJ Int. **50** (3), 455-462 (2010).
[11] A. Amadeh, B. Pahlevani, S. Heshmati-Manesh, Corros. Sci. **44** (10), 2321-2331 (2002), DOI: 10.1016/S0010-938X(02)00043-4.
[12] X. L. Xu, Z.W. Yu, S.J. Ji, J.C. Sun, Z.K. Hei, Acta Metall. Sin. – Engl. **14** (2), 109-114 (2001).
[13] F.W. Ling, D.E. Laughlin, S.C. Chang, Mater. Sci. Eng. **51** (1), 47-53 (1981), DOI: 10.1016/0025-5416(81)90105-1.
[14] K.K. Rao, H. Herman, E. Parthé, Mater. Sci. Eng.**1** (1), 162-166 (1966).
[15] L.L. Lachowicz, M.B. Lachovicz, Arch. Foundry Eng. **17** (3), 79-84 (2017), DOI: 10.1515/afe-2017-0095.
[16] A.E. Ares, L.M. Gassa, C.E. Schvezov, M.R. Rosenberger, Mater. Chem. Phys. **136** (2-3), 394-414 (2012), DOI: 10.1016/j.matchemphys.2012.06.065.
[17] C.T. Rueden, J. Schindelin, M.C. Hiner, B.E. DeZonia, A.E. Walter, E.T. Arena, K.W. Eliceirin, BMC Bioinformatics **18** (1), 529 (2017), DOI: 10.1186/s12859-017-1934-z.
[18] L. Lutterotti, S. Matthies and H. R. Wenk, ICOTOM-12, 1599 (1999).
[19] W.R. Osório, C.M. Freire, A. Garcia, J. Alloy. Compd. **397** (1-2), 179-191 (2005), DOI: 10.1016/j.jallcom.2005.01.035.